

Article

Assessment of Water-Related Ecosystem Services and Beneficiaries in the Hainan Tropical Rainforest National Park

Jeffrey Chiwukem Chiaka ^{1,2}, Qing Yang ^{3,4,*}, Yanwei Zhao ^{1,4}, Feni Agostinho ^{1,5}, Cecília M. V. B. Almeida ^{1,5}, Biagio F. Giannetti ^{1,5}, Hui Li ¹, Mingwan Wu ¹ and Gengyuan Liu ^{1,4,*}

¹ State Key Joint Laboratory of Environmental Simulation and Pollution Control, School of Environment, Beijing Normal University, Beijing 100875, China; awei1974@bnu.edu.cn (Y.Z.); feni@unip.br (F.A.); cmvbag@unip.br (C.M.V.B.A.); biafgian@unip.br (B.F.G.); lihuui@bnu.edu.cn (H.L.); 202431180023@mail.bnu.edu.cn (M.W.)

² Anambra-Imo River Basin Development Authority, Owerri PMB 1301, Nigeria

³ Advanced Interdisciplinary Institute of Environment and Ecology, Guangdong Provincial Key Laboratory of Wastewater Information Analysis and Early Warning, Beijing Normal University, Zhuhai 519087, China

⁴ Institute of Hainan National Park, Haikou 570228, China

⁵ Post-graduation Program on Production Engineering, Paulista University (UNIP), Sao Paulo 01504-000, Brazil

* Correspondence: yangqing14@mails.ucas.edu.cn (Q.Y.); liugengyuan@bnu.edu.cn (G.L.)

Abstract: Tropical rainforests are of vital importance to the environment, as they contribute to weather patterns, biodiversity and even human wellbeing. Hence, in the face of tropical deforestation, it becomes exigent to quantify and assess the contribution of ecosystem services associated with tropical rainforests to the environment and especially to the people. This study adopted a nuanced approach, different from traditional economic valuations, to estimate the water-related ecosystem services (WRESs) received by the people from 2010 to 2020 in the Hainan Tropical Rainforest National Park (HTRNP). The study focused on water yield, soil conservation, and water purification using InVEST, the SCS-CN_{GIS} model, and spatial analysis. The results show (1) significant land cover changes within the HTRNP, as forest decreased by 4433 ha and water bodies increased by 4047 ha, indicating the active presence of human activities. However, land cover changes were more pronounced within the 5 km buffer area around the HTRNP, suggesting the effectiveness of the tropical rainforest conservation efforts in place. (2) The water yield of the HTRNP in the years studied decreased by 307.03 km³, based on the water yields in 2010 and 2020, which were 5625.7 km³ and 5318.7 km³, respectively. (3) Change detection showed that runoff mitigation in the rainforest has a negative mean (−0.21), indicating a slight overall decrease in soil conservation and runoff mitigation in the rainforest from 2010 to 2020; however, the higher curve number indicates areas susceptible to surface runoff. (4) The ecological effectiveness of water purification to absorb and reduce nitrogen load was better in 2020 (145,529 kg/year), as it was reduced from 506,739 kg/year in 2010, indicating improved water quality. (5) Population growth is more pronounced in areas with high water yields. Overall, the proposed framework has shown that the water yield potential of the HTRNP can meet the water consumption demands of people and industries situated within the buffer area. However, analysis of the study shows that it does not meet the crop water requirements. This study provides insights for decision makers in identifying potential beneficiaries and the essence of effective area-based conservation measures, and the proposed framework can be applied to any area of interest, offering a different approach in ecosystem services assessment.

Keywords: tropical rainforest; land use change; human demand; ecosystem management and conservation; InVEST model; population growth



Citation: Chiaka, J.C.; Yang, Q.; Zhao, Y.; Agostinho, F.; Almeida, C.M.V.B.; Giannetti, B.F.; Li, H.; Wu, M.; Liu, G. Assessment of Water-Related Ecosystem Services and Beneficiaries in the Hainan Tropical Rainforest National Park. *Land* **2024**, *13*, 1804. <https://doi.org/10.3390/land13111804>

Academic Editor: Shicheng Li

Received: 3 September 2024

Revised: 11 October 2024

Accepted: 30 October 2024

Published: 31 October 2024



Copyright: © 2024 by the authors. Licensee MDPI, Basel, Switzerland. This article is an open access article distributed under the terms and conditions of the Creative Commons Attribution (CC BY) license (<https://creativecommons.org/licenses/by/4.0/>).

1. Introduction

Tropical rainforests provide significant ecosystem services, such as freshwater, air purification, floods mitigation, biodiversity, etc., [1,2]. However, deforestation has reduced

their area cover from 12% to less than 5% [3]. Hence, protecting the ecosystem so that it can continue to provide its services, especially water-related ecosystem services (WRESs), is a top priority. Due to the threats to the integrity of global rainforest regions, studies posit policies, such as designating areas as ‘protected’ can conserve them from further degradation [4]. Effective protected areas have proven to be beneficial to ecosystem functions, nature conservation, and improved livelihoods [5]. For instance, China, as a net importer of timber, placed a moratorium on logging in the country’s natural forest in 2015 to enable forest recovery [6]. Therefore, protected areas and other effective area-based conservation measures (OECMs), such as national parks, are initiated in view of the threats posed by population growth, urbanization, and climate change to ecosystem services (ESs) [7–9].

The establishment of national parks as a conservation measure aims to improve the ecological environment, biodiversity conservation and even ecotourism [10,11]. The United States of America was the first country to initiate a national park in 1872 for conservation purposes and for the benefit of the people. In 1979, Kainji Lake was established as the first National Park in Nigeria to protect its diverse ecosystems and biodiversity [12]. Kakadu National Park is the largest conservation reserve in Northern Australia and is known for the conservation of threatened species [13]. Itatiaia National Park (INP) in Brazil is significant for the protection of bryoflora, endemism, and threatened species [14]. Similarly, some countries, like China, have implemented ecological measures to protect ecology and biodiversity by establishing national key ecological zones, priority areas for biodiversity conservation, and natural capital restoration [15,16]. Such priority areas are located on Hainan Island, situated on the southern coast of China, due to the increasing habitat fragmentation [17].

Hainan Island is facing severe land degradation, exacerbated by the socioeconomic conditions of its inhabitants, as most locals have a low income and there is widespread poverty [18]. Such a socioeconomic status has been linked to increased land degradation [19], as poor households tend to exploit the natural resources of their immediate surroundings [20]. However, establishing national parks as a mitigation strategy has not only been seen as protecting terrestrial and coastal areas from anthropogenic activities but also as providing a conducive environment for people to benefit from nature [21–23]. In this context, the Hainan Tropical Rainforest National Park (HTRNP), one of the world’s biodiversity hotspots, established in 2021, was conceived to be an ecological pilot zone to support the conservation and provision of ecosystem services, such as clean water and soil conservation, for Hainan Island [15,24].

As a result, various studies have attempted to ascertain the environmental sustainability and ecosystem function of Hainan Island, including the tropical rainforest, which is considered a well-preserved national park in Hainan and the country in general [25]. In these studies, questionnaires, spatial weights [18], integrated valuation of ecosystem services and trade-offs (InVEST), the Carnegie–Ames–Stanford Approach (CASA) and revised universal soil loss equation (RULSE) [26], nutrient flow in food chains, environment, and resources (NUFER) [27], and even a static Bayesian network [28] have been used to model and even predict the future water quality.

Although various studies highlighted the diverse ecosystem services improvements [29] and the identification of priority areas for the restoration and optimization of ecosystem services [18,30] in the Hainan Tropical Rainforest National Park, the ecosystem service contributions to the people are understudied. This is because the evaluation of the viability of the national park without considering its natural capital demand amounts to a partial sustainability assessment. Moreover, as the designation of land as protected areas is increasing [23], knowing these areas’ effectiveness in protecting biodiversity and capacity to provide ecosystem services [31] is essential, but equally significant is considering who benefits from these reserves and how they meet various needs.

In advancing the assessment of ecosystem services, the InVEST model has been used, and it has performed well in the estimation of regulating ecosystem services, such as water yield and nutrient load [24,32,33]. Nevertheless, when using the InVEST model,

some studies may not provide details on the spatial resolution of certain variables, such as land cover. However, one study suggests that the outcome of the annual water yield from the InVEST model is determined by the spatial resolution of the digital elevation model (DEM) data [32]. Based on this concept, an innovative attempt was made in this study to resample all input data rather than just one input variable when using the InVEST model. Furthermore, while estimating soil conservation with the RUSLE model may be feasible [34], the process is cumbersome. Hence, this study aims to fill the aforementioned gaps by using finer spatial resolution of input variables when using the InVEST model for a detailed spatial outcome and a cloud-based GIS soil conservation technique that requires less computational time and can be applied at larger scale. Therefore, this study builds a framework that focuses on assessing the regulatory ecosystem services of the national park over the decade (2010–2020) preceding its designation using the InVEST model, GIS-based soil conservation services curve numbers (SCS-CN_{GIS}), and spatial analysis to identify the potential of the rainforest and its contributions to the people.

Subsequently, some studies have used a benefit transfer approach [35], which is expressed in monetary terms and may not entirely represent the direct benefits to people. Keeler et al. [36] developed a prioritization metric to estimate the ecosystem service supply (ESs) and value for an agricultural landscape. This approach considered areas in the watershed that provide greater supply and value of ecosystem services benefits to people, but did not quantify how much of it reaches people and if the ESs supply–demand ratio is sustainable or not. Moreso, the human demand clusters are omitted.

As a result of the aforementioned issues, this study proposed a nuanced approach that will reassess (i) the potential contribution of water-related ecosystem services (WRESs) in terms of soil conservation, water quantity, and purification, (ii) the associated human demand for water, and (iii) the areas that benefit from these ecosystem services, especially water yield. Hence, the novelty of this approach lies in the use of finer spatial resolution of input variables while running the InVEST model and a cloud-based GIS soil conservation technique that requires less computational time while quantifying the benefit non-monetary ecosystem services to people.

2. Methods

2.1. Study Area

Hainan Island, located between 18°10' N and 21°10' N latitude, and 108°37' E and 110°03' E longitude [37], is the second largest island off the coast of China. It has a tropical maritime monsoon climate, with an average annual temperature ranging from 22.8 °C to 25.8 °C, annual rainfall between 961 mm and 2439 mm [38], a minimum elevation of −3 m and a maximum elevation of 1840 m at Wuzhi Mountain. The island's climate, with high temperatures and abundant rainfall [39], is suitable for growing food, especially fruits and vegetables [40] and the soil type in this area is predominantly brick-red soil, which also creates favorable conditions for the growth of mangroves [41].

The Hainan Tropical Rainforest National Park is located in the central and southern mountainous regions of Hainan Island (Figure 1). The park covers a total of 4403 km² (13%) of the land area of Hainan Island [10]. As a coastal island, the ecological environment is impacted by climate change [26]. Additionally, the economic and urban development in the area have led to land fragmentation and impacted the island's ecosystem service function [26]. The digital elevation of the location and land use land cover as at the time of this study are shown in Figure 1.

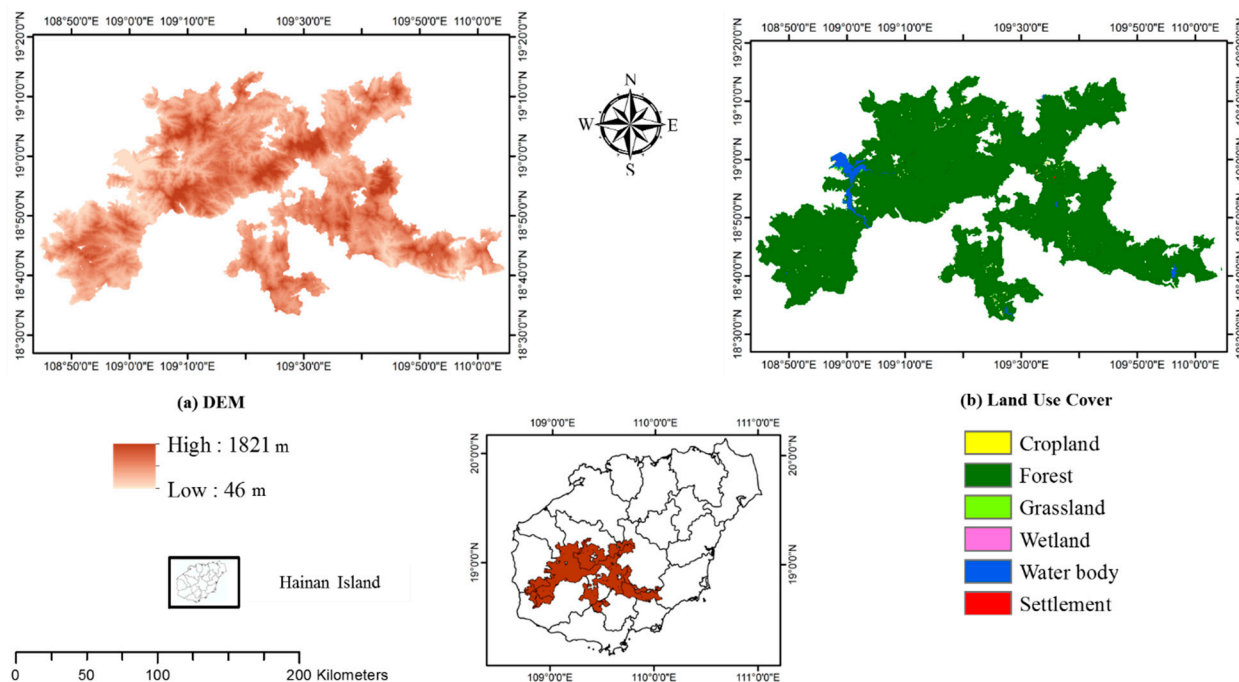


Figure 1. Showing (a) digital elevation model and (b) recent land use cover (2020) of the Hainan Tropical Rainforest National Park (HTRNP), China.

2.2. Data Source

The data used in this study mainly include two types, namely socioeconomic and ecological parameters. Socioeconomic data mainly include population and average per capita water consumption; ecological parameters mainly include land use change, precipitation, evapotranspiration, soil texture, and so on. The specific data source is listed in Table 1.

Table 1. Summary of data sources.

Data	Data Source	Resolution/Unit	Year
Demand model			
Population	Resource and Environmental Science Data (RESDC)	1000 m	2010, 2019
Average per capita water Consumption	Statista [42]	cm ³	2010, 2020
InVEST model (water yield)			
Land use cover	National Geomatics Center of China (NGCC)	30 m	2010, 2020
Precipitation	Climatic Research Unit—University of East Anglia	0.5°	2010, 2020
Evapotranspiration	Terra (MODIS) Evapotranspiration/latent heat flux	500 m	2010, 2020
Root resisting layer depth	Harmonized World Soil Database	1000 m	2013
Plant available water content	Harmonized World Soil Database	1000 m	2013
GIS-based soil conservation services curve numbers (SCS-CN _{GIS}) model (runoff mitigation)			
Land use cover	MODIS Land Cover	500 m	2010, 2020
Soil texture	OpenLandMap Soil Texture Class (USDA System)	250 m (depth)	2010, 2020
Precipitation	Climate Hazards Group InfraRed Precipitation (CHIRPS)	0.05°	2010, 2020
InVEST model (Water Purification)			
Digital Elevation Model	SRTM Digital Elevation Data	90 m	2000
Land use cover	National Geomatics Center of China (NGCC)	30 m	2010, 2020
Precipitation	Climatic Research Unit -University of East Anglia	0.5°	2010, 2020

Note: This study initiated a resampling of all input data for the InVEST model to a finer spatial resolution of 30 m.

2.3. Assessment Framework of Water-Related Ecosystem Services and Beneficiaries

The conceptual framework proposed in this study for the assessment of water-related ecosystem services (WRESs) and beneficiaries is shown in Figure 2. Figure 2 shows that the spatiotemporal variations of three water-related ecosystem services, i.e., water yield, soil conservation, and water purification, were assessed using the InVEST model, SCS-CN_{GIS} model, and spatial analysis of land use change to account for potential contributors and beneficiaries. Specifically, a land use land cover detection and change analysis was carried out to analyze the state of the rainforest.

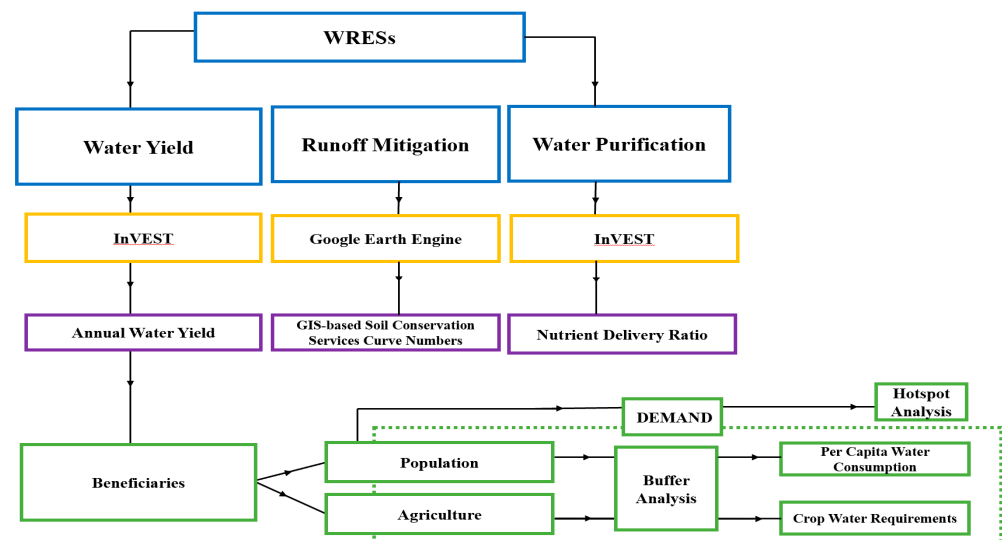


Figure 2. Assessment framework of water-related ecosystem services (WRESs) and demand.

In detail, this study utilized the InVEST model to assess annual water yield available as runoff to rivers and for human consumption. The SCS-CN_{GIS} model was applied to estimate the soil conservation/runoff mitigation services in the national park, and the InVEST nutrient delivery ratio was used to evaluate the water purification services. Lastly, hotspot and buffer analysis were initiated in the ArcGIS environment using population and agriculture as proxies to quantify the relationship between the demand for water yields within the park and their consumption outside the park [43].

It is worth noting that beneficiaries, used as a proxy for demand, are evaluated within a 5 km buffer outside the national park, as we considered the impact of the park to be more prominent in this area, while other analyses were conducted within the park itself. These assessments were carried out using InVEST 3.14, ArcGIS 10.6 software, and the Google Earth Engine cloud-based platform.

2.3.1. Water Yield Assessment

The InVEST water yield model was used to quantify water yields of different catchments or sub-catchments of an area, taking into account changes in land use, climate, and soil depth. The outcome of the water yield illustrates the total annual water yield potential that can be used for irrigation and human consumption. Furthermore, the InVEST water yield model is based on the Budyko curve and annual mean precipitation [44], and the specific calculation formula is as follows:

$$Y(x) = \left(1 - \frac{AET(x)}{P(x)}\right) \cdot P(x) \quad (1)$$

where $Y(x)$ indicates annual water yield (mm); $AET(x)$ means actual evapotranspiration for pixels x (mm); $P(x)$ refers to annual precipitation in pixels x .

To estimate the land cover, Equation (1) is further broken down as follows:

$$\frac{AET}{P(x)} = 1 + \frac{PET(x)}{P(x)} - \left[1 + \left(\frac{PET(x)}{P(x)} \right)^\omega \right]^{1/\omega} \quad (2)$$

where $PET(x)$ means potential evapotranspiration for pixels x (mm); ω refers to the coefficient of water availability for plants as a non-physical parameter that characterizes the relationship between climate and soil depth.

The coefficient of water available for plants at pixel x has the following equation:

$$\omega(x) = Z \frac{AWC(x)}{P(x)} + 1.25 \quad (3)$$

where $\omega(x)$ means the coefficient of water availability for plants in pixels x ; Z = Zhang coefficient (seasonality factor); $AWC(x)$ means the water content available to plants (mm); $P(x)$ refers to the annual precipitation in pixels x .

The Zhang coefficient represents seasonal climate factor that shows local precipitation patterns and hydrogeological characteristics determined on a scale from 1 to 10, where 1 represents a seasonal monsoon, 4 means a tropical climate, and 9 illustrates a temperate climate [45]. A value of 4 was selected for the Z coefficient in this study. Additionally, the InVEST model requires biophysical parameters for the model to calculate the annual water yield (Table 2). The study further that assumed factors, such as Root depth (mm) and Kc (ratio from 0–1), are consistent within the study period, i.e., 2010 to 2020, as these factors take a long time to change.

Table 2. Water yield biophysical parameters linked to land cover characteristics in the rainforest.

Land Use Type	Land Use Code		Root Depth		Kc		Land Cover Vegetation	
	2010	2020	2010	2020	2010	2020	2010	2020
Cropland	10	10	200	200	0.7	0.7	1	1
Forest	20	20	200	200	1	1	1	1
Grassland	30	30	200	200	0.8	0.8	1	1
Wetland	n/a	50	0	0	n/a	1	0	0
Water body	60	60	0	0	1	0.3	0	0
Settlement	80	80	0	0	0.3	0.2	0	0

2.3.2. Runoff Mitigation Assessment

This study utilized the traditional soil conservation service curve number (SCS-CN) method [46], but transformed in a geospatial environment using the Google Earth Engine to predict surface runoff during rainfall and to evaluate runoff potential in the watersheds. This accounts for more precise effects of soil properties, land cover, and antecedent moisture. The SCS-CN conceptual model is given as follows:

$$\frac{Q}{P - I_a} = \frac{(P - I_a) - Q}{S} \quad (4)$$

where Q = actual runoff (mm); $(P - I_a)$ = maximum potential runoff (mm); $(P - I_a) - Q$ = actual retention (mm); S = potential retention (mm). This is further broken down into Equation (5), as follows:

$$Q = \frac{(P - I_a)^2}{(p - I_a + S)} \quad (5)$$

where Q = discharge (mm); P = precipitation (mm); I_a = initial abstraction (mm); S = maximum potential retention (mm). Equation (5) is further broken down as follows:

$$Q = \frac{(P - I_a)^2}{(S)} \quad (6)$$

However, I_a depends on a 5-day antecedent moisture content. Therefore, under average conditions, $I_a = 0.2S$. Hence, Equation (7) is as follows:

$$Q = \frac{(P - 0.2S)^2}{(P + 0.8S)} \quad (7)$$

S can be computed as follows:

$$S = \frac{25400}{CN} - 254 \quad (8)$$

where S is in millimeters and CN is a dimensionless runoff coefficient that depends on land use, soil, and the antecedent moisture condition (AMC). Furthermore, the antecedent moisture condition (AMC), which is the soil moisture condition of the watershed, is another important factor influencing the final curve number (CN) value. This means that the higher the soil moisture condition, the higher the CN .

The antecedent moisture is defined as the relative dryness or wetness of a catchment area, which is constantly changing and has a significant influence on the runoff process [47]. Antecedent moisture can be categorized into three classes, including AMC I, which is a dry condition with five-day antecedent rainfall, i.e., the AMC is less than 13 mm. However, if the AMC is more than 28 mm, it can be a wet condition (AMC III), and if $13 \text{ mm} \leq \text{AMC} < 28 \text{ mm}$, it may be considered average (AMC II) [48]. The CN for AMC I and AMC III can be derived using the following equations:

$$CN(I) = \frac{CN(II)}{2.281 - 0.0128CN(II)} \quad (9)$$

$$CN(III) = \frac{CN(II)}{0.427 - 0.00573CN(II)} \quad (10)$$

2.3.3. Water Purification Assessment

To find out the water quality of the rainforest, the nutrient delivery ratio (NDR) component of the InVEST model is able to delineate nutrient sources from watersheds and their transport to the stream, as this study considered only surface water export. Therefore, land use and corresponding changes in the rainforest will be reflected in the water quality as non-point pollution sources. The nutrient loads are defined as follows:

$$X_{export_i} = Load_{surf,i} \times NDR_{surf,i} + Load_{subs,i} \times NDR_{subs,i} \quad (11)$$

$$X_{export_{total}} = \sum_i X_{export_i} \quad (12)$$

where, $Load_{surf,i}$ and $Load_{subs,i}$ represent the nutrient load from surface and subsurface sources, respectively, while $NDR_{surf,i}$ and $NDR_{subs,i}$ represent the nutrient delivery ratio for surface and subsurface sources, respectively.

Each computed pixel's load is modified to account for the local runoff potential that can be divided into surface and subsurface runoff. This means that nutrients are transported by surface or shallow subsurface runoff, while the subsurface accounts for nutrients transported by groundwater.

The ratio between these two types of nutrient sources is given by the parameter $proportion_{subsurface_i}$; therefore, the load ($\text{kg} \cdot \text{ha}^{-1} \cdot \text{yr}^{-1}$) for pixel i is defined as follows:

$$\left. \begin{aligned} Load_{surf,i} &= (1 - proportion_{subsurface_i}) \times modified_{load_i} \\ Load_{subsurf,i} &= proportion_{subsurface_i} \times modified_{load_i} \end{aligned} \right\} \quad (13)$$

$$modified_{load_i} = load_i \times RPI_i \quad (14)$$

$$RPI_i = \frac{RP_i}{RP_{av}} \quad (15)$$

where RPI_i is the runoff potential index for pixel i , RP_i is the nutrient runoff proxy for runoff on pixel i , and RP_{av} is the average RP over the entire area.

The delivery ratios ($NDR_{surf,i}$ and $NDR_{subs,i}$) are computed based on the concept of the nutrient delivery ratio. However, as mentioned earlier, this study considered only surface water export, given as follows.

(i) Surface NDR

The surface NDR is the product of a delivery factor, representing the ability of downstream pixels to transport nutrients without retention, and a topographic index, representing the position on the landscape. For pixel i , Equation (15) is as follows:

$$NDR_{surf,i} + NDR_{0,i} = \left(1 + \exp\left(\frac{IC_i - IC_0}{k}\right)\right)^{-1} \quad (16)$$

where IC_0 and k are calibration parameters; IC_i is a topographic index; $NDR_{0,i}$ is based on the maximum retention efficiency of the land between a pixel and the stream. Equations (17) and (18) are as follows:

$$NDR_{0,i} = 1 - eff'_i \quad (17)$$

$$eff'_i = \begin{cases} eff_{LULC_j} \cdot (1 - s_i) & \text{if } down_i \text{ is a stream pixel} \\ eff'_{down_i} \cdot s_i + eff_{LULC_j} \cdot (1 - s_i) & \text{if } eff_{LULC_j} > eff'_{down_i} \\ eff'_{down_i} & \text{otherwise} \end{cases} \quad (18)$$

where eff_i is retention efficiency for pixel i ; eff_{LULC} is the maximum retention efficiency that $LULC_j$ can reach; eff'_{down_i} is the effective downstream retention on the pixel directly downstream from pixel i , and s_i is the step factor, defined as follows:

$$s_i = \exp\left(\frac{1 - 5l_{i_{down}}}{l_{LULC_i}}\right) \quad (19)$$

where $l_{i_{down}}$ is the length of the flow path from pixel i to its downstream neighbor; l_{LULC_i} is the LULC retention length of the land cover type on pixel i .

IC is the index of connectivity, as follows:

$$IC = \log_{10}\left(\frac{D_{up}}{D_{dn}}\right) \quad (20)$$

$$D_{up} = \overline{S}\sqrt{A}, \quad D_{dn} = \sum_i \frac{d_i}{S_i} \quad (21)$$

where \overline{S} (m/m) is the average slope gradient of the upslope contributing area; A (m²) is the upslope contributing area, and d_i (m) is the length of the flow path along the pixel i .

Due to paucity of nutrient load data for the Hainan tropical rainforest, the biophysical parameters for 2010 were generated from the 2017 land cover nitrogen load from the framework of coupled human and natural systems nitrogen cycling model spatial distribution (CHANS-SD) [49]. The 2020 data on the nitrogen load of Hainan Island were collated from Li et al. [18].

Furthermore, the biophysical indicator 'eff_nutrient' (range 0–1) represents the maximum nutrient retention efficiency, which is the maximum proportion of the nutrient that is retained on the LULC. Furthermore, crit_len_nutrient (meters) is the distance for which it is assumed that the LULC retains the nutrient at its maximum capacity (Table 3).

Table 3. NDR biophysical parameters linked to land cover characteristics in the HTRNP.

Land Use Type	Land Cover Code		Nitrogen Load		eff_Nutrient		crit_len_Nutrient	
	2010	2020	2010	2020	2010	2020	2010	2020
Cropland	10	10	49.5	53.5	0.25	0.25	30	30
Forest	20	20	12	3	0.8	0.8	300	300
Grassland	30	30	10.8	7	0.5	0.5	150	150
Wetland	-	50	-	15	0	0.05	0	15
Water body	60	60	10.7	0.3	0.02	0.02	150	150
Settlement	80	80	1	13.8	0.05	0.05	15	15

2.3.4. Water Yield Demand Assessment

This is a two-pronged approach in which demand is measured from the perspective of water consumption and hotspot areas. Therefore, three indicators are considered, namely population, built-up area, including the number of people and housing (residential, commercial, and industrial usage), and the cropland area outside a buffer zone of 5 km around the national park. The reason to establish a buffer area of 5 km is to account for the human demands within a specified zone outside the national park.

Hence, to determine the water consumption demand of the people within the 5 km buffer from the rainforest, the average per capita water consumption data were used. To quantify industrial use, this study used spatial zonal statistics on the land cover images. For estimating the cropland water needs, the crop water requirement for rice, maize, and sugarcane [50] was adopted in this study, as these crops are commonly cultivated in Hainan, while population clusters were used to determine the demand hotspots.

3. Results

3.1. Land Use Cover Changes from 2010 to 2020 in the HTRNP

From the land cover classification, the tropical rainforest consists of six land cover classes, namely cropland, forest, grassland, wetland, water body, and settlements. The predominant land cover class based on abundance and extent is forest cover, which decreased in 2020 (Table 4). However minimal, the land cover transition matrix indicated deforestation compared to the total forest area, as about 424.9 ha of forests were converted to croplands. This was followed by grassland (214.8 ha), wetlands (18.5 ha), water bodies (4083.3 ha), and settlements (56.7 ha). Overall, aside from the observed reduction in forest-covered areas, other land covers showed varying degrees of expansion from 2010 to 2020 (Table 4). The 5 km buffer area outside the rainforest showed similar land cover and changes but with a high rate of forest loss. Forest had the highest loss rate at 17,363 ha, while cropland gained 12,686 ha. Other notable increases were settlements with 2618 ha and water bodies with 1842 ha (Table 4).

Table 4. Land use and cover change inside and surrounding Hainan Tropical Rainforest National Park (HTRNP).

Land Use Type	HTRNP (Ha)			Buffer Zone (Ha)		
	2010	2020	Change	2010	2020	Change
Cropland	2575	2671	96	50,869	63,555	12,686
Forest	421,625	417,192	−4433	302,727	285,364	−17,363
Grassland	21	257	236	393	527	135
Wetland	-	19	19	-	-	-
Water body	2536	6582	4047	1586	3428	1842
Settlement	79	112	33	1074	3692	2618
Bare land	-	-	-	91	167	76

3.2. Water Yield

The annual water yield of the HTRNP was 5625.7 km³ in 2010 and 5318.7 km³ in 2020, with the distribution pattern shown in Figure 3. As such, the water yield declined by 307.03 km³ within a decade. The spatial distribution highlighted the main water-producing areas, which are located in the northeast and southeast of the rainforest, i.e., Mao Rui, Wuzhi Shan, Diaoluo Shan, and some parts of the Limu Shan catchment area. The moderate water yield areas are located at the center, which comprises the BaiWang Ling and YingGe Ling catchment areas. Also, low water yield areas are seen to the southwest of the rainforest, where the JianFeng Ling catchment is located.

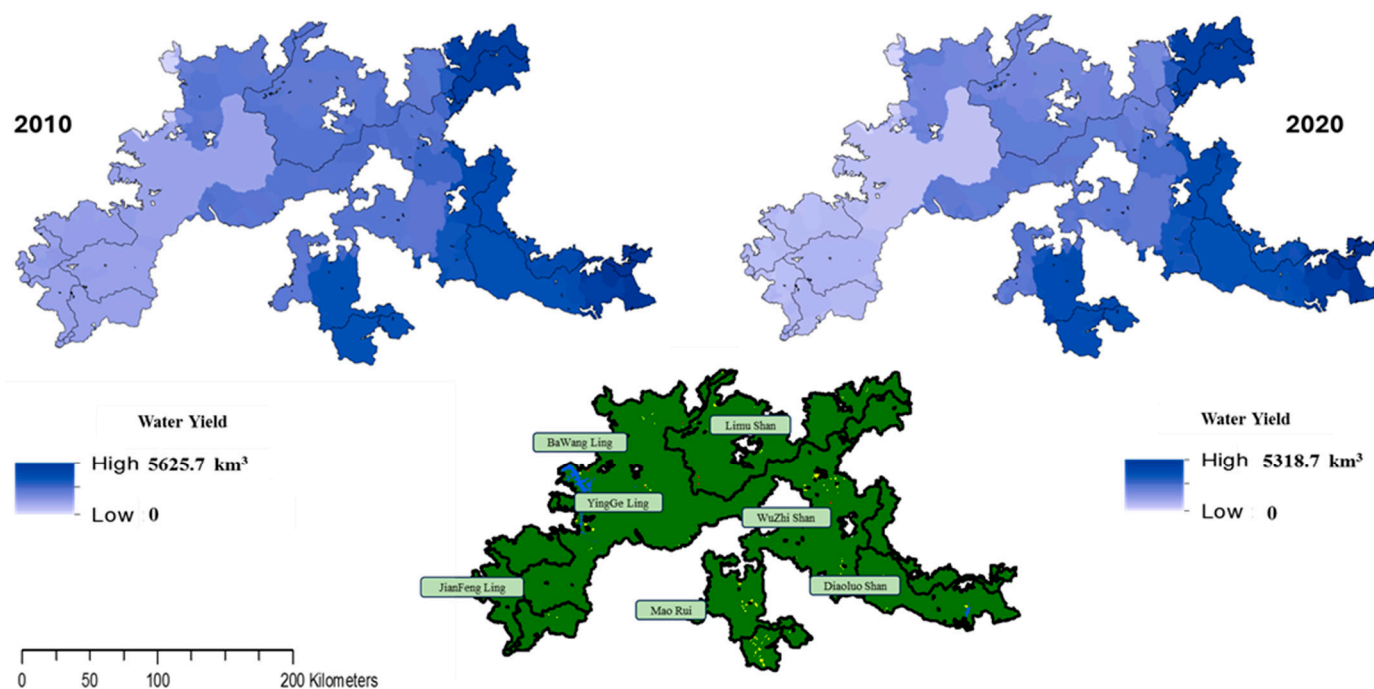


Figure 3. Spatial pattern of water yield distribution within the Hainan Tropical Rainforest National Park in 2010 and 2020.

3.3. Soil Conservation and Runoff Mitigation

The curve number model shows that the area with a lower curve number has greater infiltration and lower runoff potential and vice versa. From the associated curve numbers, the central areas of the rainforest showed consistency in low runoff, the east and southeast areas had high runoff, and the south and northwest areas exhibited the same high runoff potential, as shown in Figure 4. Further breakdown of the analysis indicates a decrease in rainfall volume in 2020 that implies a lower amount of surface runoff in 2020 than in 2010 (Figure 4). This means the effective rainfall, which is estimated after accounting for losses due to evaporation and infiltration, showed a reduction. This further indicates that less rainfall contributed to runoff in 2020 than in 2010. Lastly, the runoff ratio, which is estimated by dividing the runoff by the total rainfall of each year, also decreased from 2010 to 2020. This highlights a reduced amount of rainfall constituting surface runoff in 2020 compared to 2010. Succinctly, the runoff mitigation of the rainforest suggests a shift to more water retention and reduced surface runoff in the national park. This indicates a higher amount of water infiltration and a reduction in surface runoff, but the probability of runoff is higher in most parts based on the curve numbers, which may be related to topography.

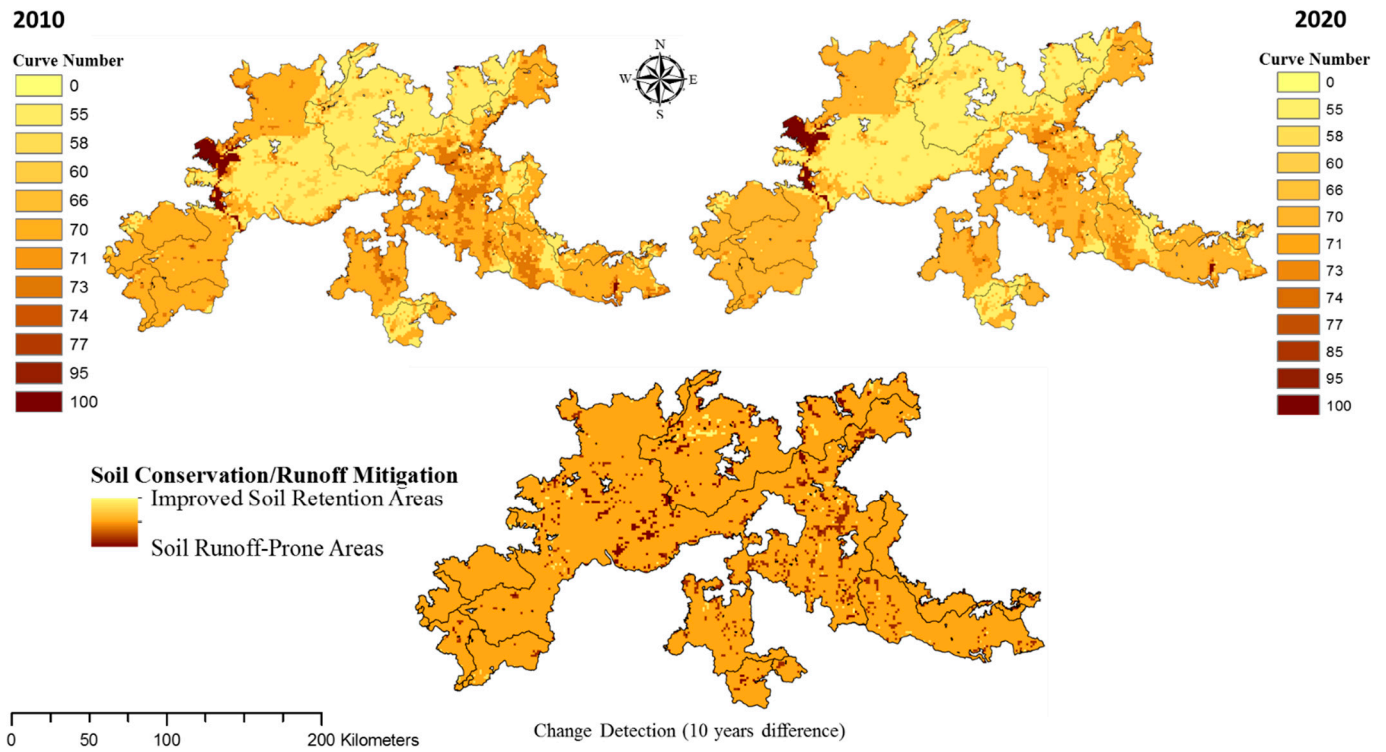


Figure 4. Spatial distribution of soil conservation/runoff reduction based on curve number in the Hainan Tropical Rainforest National Park of Hainan.

3.4. Nutrient Load and Export

The higher the total nitrogen exports (TN) per unit area, the weaker the water purification capacity of the rainforest. This is because land cover serves as a purifier for nitrogen loads. The NDR results show a significant decrease in exported nitrogen load, as the total nitrogen exported from the watershed by surface flow from the rainforest in 2010 and 2020 was 506,739 kg/year and 145,529 kg/year, respectively (Figure 5). Furthermore, the central area of the rainforest had high nitrogen loads compared to many of the four peripheral areas.

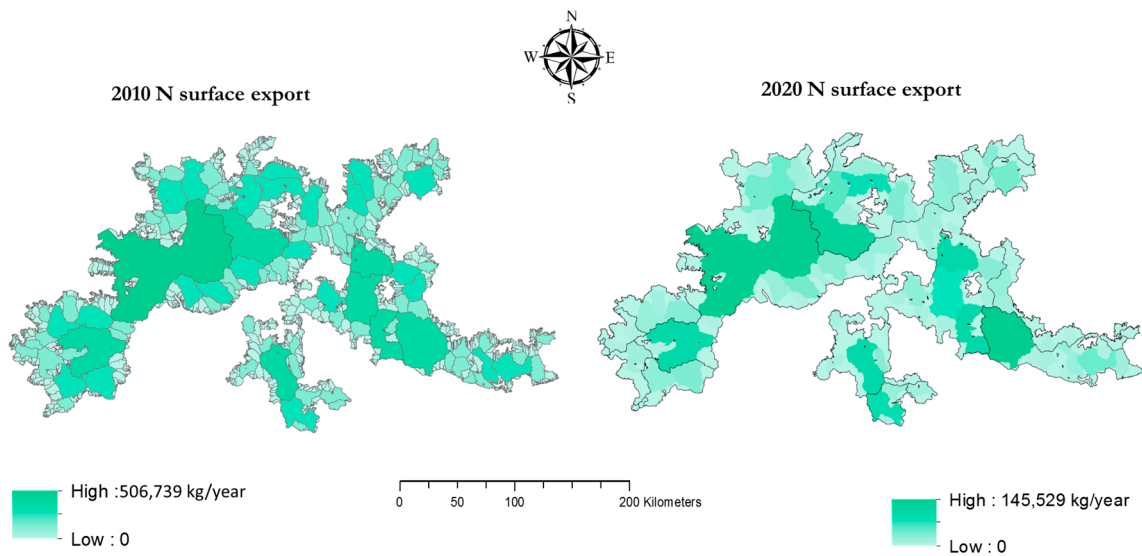


Figure 5. Total surface nitrogen export in the Hainan Tropical Rainforest National Park in 2010 and 2020.

3.5. Water Supply and Consumption

Based on the per capita water consumption in China of 450.2 cm³ in 2010 as a benchmark for the water intake of Hainan residents, the water demand of the total population (1238 people) extrapolated from the raster data and living within the 5 km buffer around the national park was 0.557 km³. In 2019, the water demand of the population (1459 people), calculated from a per capita water consumption of 411.9 cm³ was 0.624 km³. We would like to point out that due to computation errors in the population data for 2020, we have taken the data for 2019 into account. The water supply from the national park could, therefore, adequately meet their needs, as the water yield in 2010 and 2020 amounted to 5625.7 km³ and 5318.7 km³, respectively.

Spatial zonal statistics within the 5 km buffer provide the water volume usage of the land use covers. This is achieved by overlaying the land use cover with the water yield within the 5 km buffer to see how much water volume consumed by each land use cover, with particular emphasis on built-up areas, which represents residential, commercial, and industrial areas. The results indicated that built-up areas' mean water volume usage increased from 102.162 km³ in 2010 to 106.618 km³ in 2020. This represented the highest water usage after water bodies (Figure 6). Nevertheless, the water volume demand can be met within the 5 km buffer, despite the water yield being lower than that of the rainforest, which was 4953.56 km³ in 2010 and 4710.48 km³ in 2020.

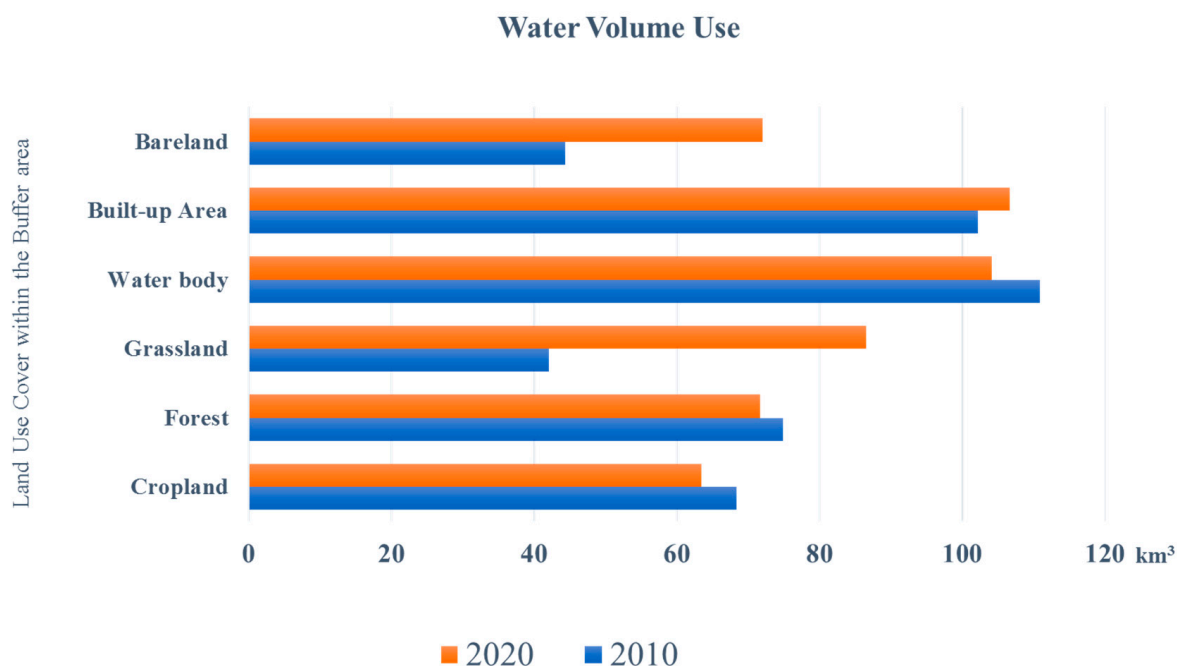


Figure 6. Water volume usage as a proxy of water demand within the 5 km buffer around the Hainan Tropical Rainforest National Park.

The water requirements to cultivate crops were multiplied by the 2010 total cropland area, and their results were rice (138,718 km³), maize (33,103 km³), and sugarcane (38,789 km³). However, in 2020, the total cropland area expanded, and therefore, with an assumption that the crop water requirement is constant, the crops will required the following: rice (173,379 km³), maize (41,375 km³), and sugarcane (48,493 km³). The total water requirements in 2010 (210,610 km³) and 2020 (263,247 km³) were higher than the available total water yield emanating from the national park. Moreover, the water yields available in the buffered area, as estimated, cannot cater to the crop water needs (the volume of water yield in the 5 km buffer area was 4953.5 km³ in 2010 and 4710.4 km³ in 2020).

It is worth noting that the hotspot analysis indicated that the population's demand for water-related ecosystems, particularly water consumption, was more notable towards

the southeast. The population in the northeast region of the rainforest remained consistent for lower demand (cold spot), while the southwest area of the rainforest, with low water yields, had lower demand (cold spot) (Figure 7).

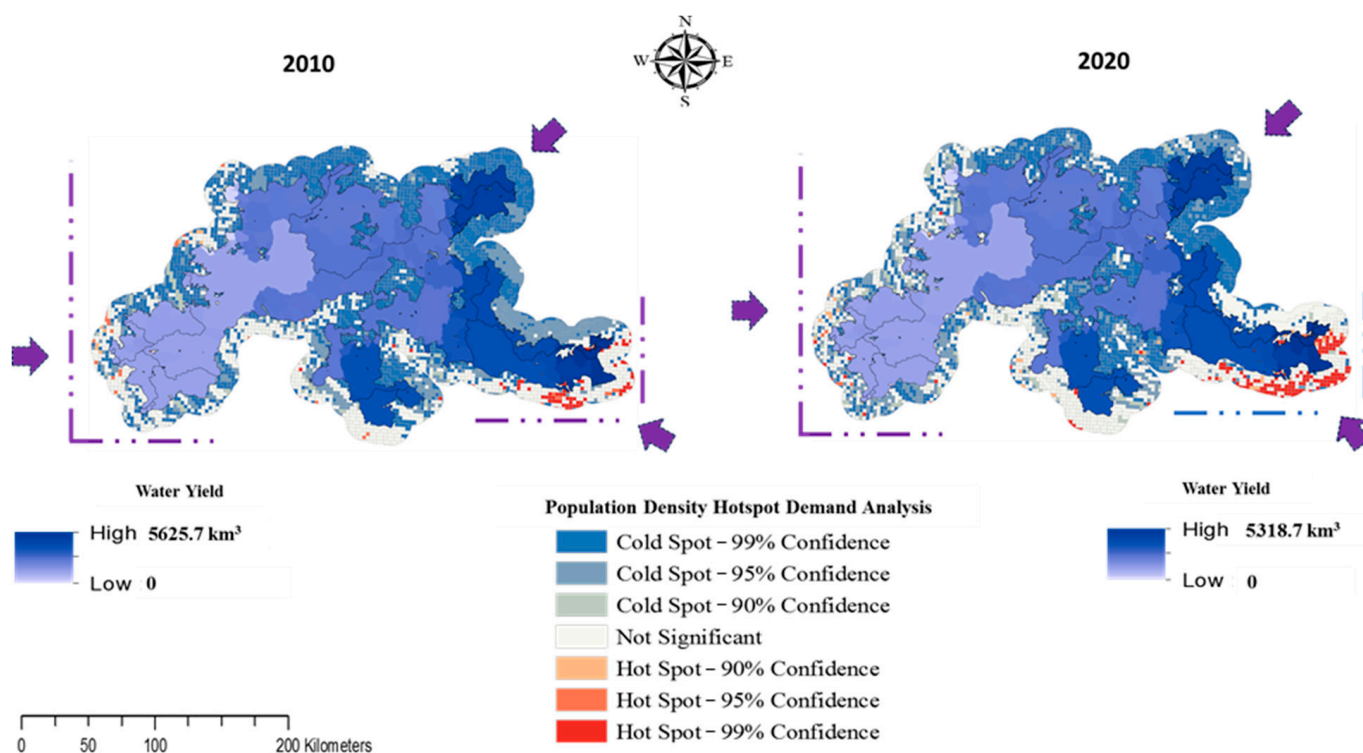


Figure 7. Population demand intensity for water in the Hainan Tropical Rainforest National Park in 2010 and 2020.

4. Discussion

As studies consider ecosystem service values, the assessment of direct benefits to the people are not adequately highlighted, or are often overlooked, especially WRESs. However, these factors are crucial for decision and policymaking. This study provided a framework for the spatial analysis of WRESs' potential and received benefits by the people from the tropical rainforest national park on Hainan Island. There is no unified approach to quantify ESs, but using the methods outlined in the framework, this study has provided a spatially explicit and non-monetary approach to ascertain the direct benefits of ESs; in this case, the benefits of WRESs to the people, rather than from a standpoint of economic valuation [51], as not all ESs can be translated into economic terms [52,53].

4.1. WRESs in the HTRNP

The study highlighted the WRESs' potential and the received contribution of the national park to the people. As previous studies have noted, land cover has influences on the hydrological cycle [54,55], and the national park has had minimal land cover changes, particularly forest cover. This is essential, as forested areas have been shown to enhance infiltration and soil physical properties [44]. This further implies that conservation efforts are effective, as land use management is crucial in ecosystem functions [56,57].

The water yield suggests that the rainforest habitat is productive. The reduction of 307.03 km³ in water yield over a decade in the HTRNP is not so drastic, given the size of the watershed and the fact that the park has a stepped terrain structure that is high in the middle and low on all sides, indicating the tendency for runoff in some areas of the national park into nearby rivers and water bodies. Additionally, this is plausible due to climate and land use change impacting the hydrological cycle, which in turn influences the changes in water yield [44,58,59].

The soil conservation and runoff mitigation of the rainforest suggest an adequate contribution to groundwater resources and plant water, as there was a reduction in surface runoff in 2020 compared to 2010. Vegetation influences evapotranspiration and infiltration rate and, in turn, affects the runoff quantity of a watershed [60,61]. Nevertheless, the curve number model has highlighted areas with a propensity for surface runoff.

The effectiveness of water purification depends on the ability of the land use cover to absorb and remove the nitrogen load. Therefore, the water purification potential of the national park improved, as it exported less nitrogen in 2020 compared to 2010. Various types of land cover contributed to the nitrogen load exported to water bodies, and special attention is needed to monitor land cover expansion, as some land cover classes have been identified to contribute more of a nitrogen load than others. For instance, cropland has been a major contributor to high pesticide and chemical fertilizer loads, followed by settlements and water bodies [62]. Consequently, these land covers excluding forest, were also observed to have expanded outside (the buffer) of the rainforest, which suggests their contributory nitrogen loading of water bodies other than the ones flowing from the rainforest. However, the reduced nitrogen load in 2020 indicates an improved rainforest habitat quality capable of nitrogen retention capacity.

4.2. Water Demand Situation of the HTRNP

In terms of demand, the per capita water consumption of the people and built-up areas usage in the buffer zone can be met by the water supply from the national park and even within the 5 km buffer zone, without raising water stress concerns, compared to some basins in the Mediterranean region [63]. However, with the Hainan Free Trade Port increase in revenues in 2023 [64], more industrialization is expected in the region, which places more demand on the water supply. In addition, extensive agriculture, as observed with the increased cropland, indicates cultivation of crops, which, as seen in this study, require optimum water for their growth. Hence, crop water management should be considered, as the water demand for rice, maize, and sugarcane exceeded the water yield of the national park and that of the buffered area. This aspect is crucial, as ecosystem service supply should meet demands to avoid unsustainable utilization of its resources [56]. Furthermore, crops grown in China use excessive fertilizer to obtain high yields, leading to environmental degradation [65].

From the hotspot analysis, the study has shown the natural tendency of population growth trending towards where water is abundant to cater to their needs and wellbeing compared to areas with less water. This implies that land use land cover changes will increase especially built-up areas and cropland land covers within the vicinity of abundant water. This raises concern for present and future sustainable natural resource utilization and the essence of effective area-based conservation measures.

4.3. The Contributions, Limitations, and Prospects of This Study

This study uses a framework to look at the supply and realized contribution of a national park to human wellbeing. The proposed model provides clarity to decision-makers, as well as being able to identify potential beneficiaries. In addition, to using finer spatial resolutions as input variables in the InVEST model, the study applied an innovative method involving remote sensing to calculate the curve number and assess the runoff mitigation from 2010 to 2020. It also used spatial analysis to determine the benefits of the national park to the people.

The limitation of this study is due to the paucity of nutrient load data for the Hainan Tropical Rainforest, as the biophysical parameters for 2010 were obtained from the 2017 coupled human and natural systems nitrogen cycling model spatial distribution (CHANS-SD) to quantify nitrogen load in China against the land use cover for 2010. Also, the InVEST and the GIS-based soil conservation model had a different land cover spatial resolution, which may influence their pixelated outcome and subsequent interpretation. Furthermore, the demand for ecosystem services assumes that the crop demand is constant in the years

studied, which may also affect the results. A further study is proposed to consider the ecosystem service contribution after its designation as a national park. Also, the study of areas considered beneficial to people within a buffer area of more or less than 5 km could provide a different result.

5. Conclusions

Ecosystem services have been defined as the benefits people obtain either directly or indirectly from ecological systems. However, these benefits will deteriorate without effective management in place. Therefore, this study highlighted the water-related ecosystem services (WRESs) of the HTRNP, and how its water yield, surface runoff mitigation, and water purification (nitrogen load export) improved from 2010 to 2020, prior to its designation.

Specifically, the water yield volume is prolific; however, a high-water volume demand from crops and the observed decline in water yield in a span of 10 years raise concern about the impacts of land use and climate change on the water cycle.

This study presented an outcome that indicates the ecological function of the rainforest is adequate in terms of its WRESs and water consumption. Still, continuous effective management and monitoring of the park is essential as population growth and subsequent human demand may impact the national park water yielding and purification functions, even from adjoining areas. Therefore, land use and water management must be designed to meet human needs without overburdening ecosystem services. Overall, applying the proposed model to any area of interest provides clarity to decision makers' and enable them to identify potential beneficiaries.

Author Contributions: Conceptualization, J.C.C., Q.Y. and G.L.; Methodology, J.C.C., Q.Y., M.W. and G.L.; Software, J.C.C., F.A. and M.W. Validation, J.C.C., Y.Z., C.M.V.B.A. and G.L.; Formal analysis, J.C.C., C.M.V.B.A. and G.L.; Investigation, Q.Y. and B.F.G.; Resources, Y.Z., B.F.G., H.L. and G.L.; Data curation, Q.Y. and H.L.; Writing—original draft, J.C.C. and G.L.; Writing—review and editing, Q.Y., F.A. and G.L.; Visualization, J.C.C.; Supervision, Q.Y. and G.L.; Project administration, G.L.; Funding acquisition, G.L. All authors have read and agreed to the published version of the manuscript.

Funding: This work is supported by the Research project of Hainan Institute of National Park (No. KY-23ZK02), the National Natural Science Foundation of China (No. 52070021), and the Guangdong Basic and Applied Basic Research Foundation (No. 2024A1515012221).

Data Availability Statement: All the data will be provided on request.

Conflicts of Interest: The authors declare no conflict of interest.

References

1. Ferraz, S.F.; Ferraz, K.M.; Cassiano, C.C.; Brancalion, P.H.S.; da Luz, D.T.; Azevedo, T.N.; Tambosi, L.R.; Metzger, J.P. How good are tropical forest patches for ecosystem services provisioning? *J. Landsc. Ecol.* **2014**, *29*, 187–200. [CrossRef]
2. Ambe, B.; Onnoghen, U. Ecosystems Services of the Tropical Rain Forest Environment: Lessons from the Cross River National Park, Nigeria. *J. Geosci. Environ. Prot.* **2019**, *7*, 1–10. [CrossRef]
3. Brandon, K. *Ecosystem Services from Tropical Forests: Review of Current Science—Working Paper 380*; Center for Global Development: Washington, DC, USA; London, UK, 2014.
4. Corlett, R.T.; Primack, R.B. Tropical Rainforest Conservation: A Global Perspective. In *Tropical Forest Community Ecology*; Carson, W.P., Schnitzer, S.A., Eds.; Blackwell Science: Hoboken, NJ, USA, 2008.
5. IUCN. Effective Protected Areas. Available online: <https://www.iucn.org/our-work/topic/effective-protected-areas> (accessed on 1 January 2024).
6. Dai, L.; Li, S.; Zhou, W.; Qi, L.; Zhou, L.; Wei, Y.; Li, J.; Shao, G.; Yu, D. Opportunities and challenges for the protection and ecological functions promotion of natural forests in China. *For. Ecol. Manag.* **2018**, *410*, 187–192. [CrossRef]
7. Arowolo, A.O.; Deng, X.; Olatunji, O.A.; Obayelu, A.E. Assessing changes in the value of ecosystem services in response to land-use/land-cover dynamics in Nigeria. *Sci. Total. Environ.* **2018**, *636*, 597–609. [CrossRef] [PubMed]
8. Hassan, Z.; Shabbir, R.; Ahmad, S.S.; Malik, A.H.; Aziz, N.; Butt, A.; Erum, S. Dynamics of land use and land cover change (LULCC) using geospatial techniques: A case study of Islamabad Pakistan. *SpringerPlus* **2016**, *5*, 812. [CrossRef]
9. Abd El-Hamid, H.T.; Mustafa, E.K.; Osman, H.E. An evaluation of ecosystem services as a result of land use changes in inland and coastal areas: A comparative study of Beijing and Freetown. *J. Coast. Cons.* **2022**, *26*, 76. [CrossRef]

10. Li, L.; Tang, H.; Lei, J.; Song, X. Spatial autocorrelation in land use type and ecosystem service value in Hainan Tropical Rain Forest National Park. *Ecol. Indic.* **2022**, *137*, 108727. [[CrossRef](#)]
11. Wang, S.; Song, S.; Shi, M.; Hu, S.; Xing, S.; Bai, H.; Xu, D. China's National Park Construction Contributes to Carbon Peaking and Neutrality Goals. *Land* **2023**, *12*, 1402. [[CrossRef](#)]
12. Marguba, L.B. The Gashaka Primate Project—Nigerias National Park, Gashaka—Gumti National Park, Nigeria and Department of Anthropology, University College London. 2005. Available online: <https://www.ucl.ac.uk/gashaka/Nigeria/> (accessed on 1 January 2024).
13. Banfai, D.S.; Bowman, D.M.J.S. Forty years of lowland monsoon rainforest expansion in Kakadu National Park, Northern Australia. *Biol. Conserv.* **2006**, *131*, 553–565. [[CrossRef](#)]
14. da Costa, D.P.; dos Santos, N.D.; de Rezende, M.A.; Buck, W.R.; Schäfer-Verwimp, A. Bryoflora of the Itatiaia National Park along an elevation gradient: Diversity and conservation. *Biodivers. Conserv.* **2015**, *24*, 2199–2212. [[CrossRef](#)]
15. Zhai, J.; Hou, P.; Cao, W.; Yang, M.; Cai, M.; Li, J. Ecosystem assessment and protection effectiveness of a tropical rainforest region in Hainan Island, China. *J. Geogr. Sci.* **2018**, *28*, 415–428. [[CrossRef](#)]
16. Ouyang, Z.; Zheng, H.; Xiao, Y.; Polasky, S.; Liu, J.; Xu, W.; Wang, Q.; Zhang, L.; Xiao, Y.; Rao, E.; et al. Improvements in ecosystem services from investments in natural capital. *Science* **2016**, *352*, 1455–1459. [[CrossRef](#)] [[PubMed](#)]
17. Lei, J.; Chen, Y.; Li, L.; Chen, Z.; Chen, X.; Wu, T.; Li, Y. Spatiotemporal change of habitat quality in Hainan Island of China based on changes in land use. *Ecol. Indic.* **2022**, *145*, 109707. [[CrossRef](#)]
18. Li, R.; Zheng, H.; Polasky, S.; Hawthorne, P.L.; O'Connor, P.; Wang, L.; Li, R.; Xiao, Y.; Wu, T.; Ouyang, Z. Ecosystem restoration on Hainan Island: Can we optimize for enhancing regulating services and poverty alleviation? *Environ. Res. Lett.* **2020**, *15*, 084039. [[CrossRef](#)]
19. Masron, T.A.; Subramaniam, Y. Does Poverty Cause Environmental Degradation? Evidence from Developing Countries. *J. Poverty* **2019**, *23*, 44–64. [[CrossRef](#)]
20. Barbier, E.B.; Hochard, J.P. Land degradation and poverty. *Nat. Sustain.* **2018**, *1*, 623–631. [[CrossRef](#)]
21. Watson, J.E.M.; Dudley, N.; Segan, D.B.; Hockings, M. The performance and potential of protected areas. *Nature* **2014**, *515*, 67–73. [[CrossRef](#)]
22. Tang, X. The establishment of national park system: A new milestone for the field of nature conservation in China. *Int. J. Geoheritage Parks* **2020**, *8*, 195–202. [[CrossRef](#)]
23. Kalinauskas, M.; Shuhani, Y.; Pinto, L.V.; Inácio, M.; Pereira, P. Mapping ecosystem services in protected areas. A systematic review. *Sci. Total Environ.* **2024**, *912*, 169248. [[CrossRef](#)]
24. Lin, X.; Fu, H. Optimization of tropical rainforest ecosystem management: Implications from the responses of ecosystem service values to landscape pattern changes in Hainan Tropical Rainforest National Park, China, over the past 40 years. *Front. For. Glob. Chang.* **2023**, *6*, 1242068. [[CrossRef](#)]
25. Wang, H.; Zeng, Y. Policy Optimization for Hainan Tropical Rainforest National Park Based on Quantitative Comparison of Regional Policies of Free Trade Port Areas. *Front. Environ. Sci.* **2022**, *10*, 891432. [[CrossRef](#)]
26. Geng, J.; Yuan, M.; Xu, S.; Bai, T.; Xiao, Y.; Li, X.; Xu, D. Urban Expansion Was the Main Driving Force for the Decline in Ecosystem Services in Hainan Island during 1980–2015. *Int. J. Environ. Res. Public Health* **2022**, *19*, 15665. [[CrossRef](#)] [[PubMed](#)]
27. Liang, X.; He, Y.; Zhu, L.; Fan, S.; Zou, Y.; Ye, C. Nitrogen and phosphorus emissions to water in agricultural crop-animal systems and driving forces in Hainan Island, China. *Environ. Sci. Pollut. Res.* **2022**, *29*, 85036–85049. [[CrossRef](#)] [[PubMed](#)]
28. Ma, J.; Chen, Q.; Wu, X.; Paerl, H.W.; Brookes, J.D.; Li, G.; Zeng, Y.; Wang, J.; Chen, J.; Qin, B. The effects of socioeconomic activities on water quality in Hainan Island, south China. *Environ. Sci. Pol. Res.* **2023**. [[CrossRef](#)]
29. Yao, X.; Zhou, L.; Wu, T.; Yang, X.; Ren, M. Ecosystem services in National Park of Hainan Tropical Rainforest of China: Spatiotemporal dynamics and conservation implications. *J. Nat. Conserv.* **2024**, *80*, 126649. [[CrossRef](#)]
30. Liu, H.; Zhang, G.; Li, T.; Ren, S.; Chen, B.; Feng, K.; Li, W.; Zhao, X.; Qin, P.; Zhao, J. Importance of ecosystem services and ecological security patterns on Hainan Island, China. *Front. Environ. Sci.* **2024**, *12*, 1323673. [[CrossRef](#)]
31. Palomo, I.; Martín-López, B.; Potschin, M.; Haines-Young, R.; Montes, C. National Parks, buffer zones and surrounding lands: Mapping ecosystem service flows. *Ecosyst. Serv.* **2013**, *4*, 104–116. [[CrossRef](#)]
32. Gashaw, T.; Worqlul, A.W.; Dile, Y.T.; Sahle, M.; Adem, A.A.; Bantider, A.; Teixeira, Z.; Alamirew, T.; Meshesha, D.T.; Bayable, G. Evaluating InVEST model for simulating annual and seasonal water yield in data-scarce regions of the Abbay (Upper Blue Nile) Basin: Implications for water resource planners and managers. *Sustain. Water Resour. Manag.* **2022**, *8*, 170. [[CrossRef](#)]
33. Wei, P.; Chen, S.; Wu, M.; Deng, Y.; Xu, H.; Jia, Y.; Liu, F. Using the InVEST Model to Assess the Impacts of Climate and Land Use Changes on Water Yield in the Upstream Regions of the Shule River Basin. *Water* **2021**, *13*, 1250. [[CrossRef](#)]
34. Thapa, P. Spatial estimation of soil erosion using RUSLE modeling: A case study of Dolakha district, Nepal. *Environ. Syst. Res.* **2020**, *9*, 15. [[CrossRef](#)]
35. Troy, A.; Wilson, M.A. Mapping ecosystem services: Practical challenges and opportunities in linking GIS and value transfer. *Ecol. Econ.* **2006**, *60*, 435–449. [[CrossRef](#)]
36. Keeler, B.L.; Dalzell, B.J.; Gourevitch, J.D.; Hawthorne, P.L.; Johnson, K.A.; Noe, R.R. Putting people on the map improves the prioritization of ecosystem services. *Front. Ecol. Environ.* **2019**, *17*, 151–156. [[CrossRef](#)]

37. Zheng, H.; Wang, L.; Peng, W.; Zhang, C.; Li, C.; Robinson, B.E.; Wu, X.; Kong, L.; Li, R.; Xiao, Y.; et al. Realizing the values of natural capital for inclusive, sustainable development: Informing China's new ecological development strategy. *Proc. Natl. Acad. Sci. USA* **2019**, *116*, 8623–8628. [[CrossRef](#)] [[PubMed](#)]
38. Zhang, P.; Ruan, H.; Dai, P.; Zhao, L.; Zhang, J. Spatiotemporal river flux and composition of nutrients affecting adjacent coastal water quality in Hainan Island, China. *J. Hydrol.* **2020**, *591*, 125293. [[CrossRef](#)]
39. Chen, L.; Wang, W.; Zhang, Y.; Lin, G. Recent progresses in mangrove conservation, restoration and research in China. *J. Plant Ecol.* **2009**, *2*, 45–54. [[CrossRef](#)]
40. Tingyu, L.; Hong, X.; Liu, S.; Wu, X.; Fu, S.; Liang, Y.; Li, J.; Li, R.; Zhang, C.; Song, X.; et al. Cropland degradation and nutrient overload on Hainan Island: A review and synthesis. *Environ. Pollut.* **2022**, *313*, 120100.
41. Richards, D.R.; Friess, D.A. Rates and drivers of mangrove deforestation in Southeast Asia, 2000–2012. *Proc. Natl. Acad. Sci. USA* **2016**, *113*, 344–349. [[CrossRef](#)]
42. Statista. Average per Capita Water Consumption in China 2010–2020. Available online: <https://www.statista.com/statistics/279679/average-per-capita-water-consumption-in-china/> (accessed on 10 April 2024).
43. Wolff, S.; Schulp, C.J.E.; Verburg, P.H. Mapping ecosystem services demand: A review of current research and future perspectives. *Ecol. Indic.* **2015**, *55*, 159–171. [[CrossRef](#)]
44. Ningrum, A.; Setiawan, Y.; Tarigan, S.D. Annual Water Yield Analysis with InVEST Model in Tesso Nilo National Park, Riau Province. *IOP Conf. Ser. Earth Environ. Sci.* **2022**, *950*, 012098. [[CrossRef](#)]
45. Kim, S.-w.; Jung, Y.-y. Application of the InVEST Model to Quantify the Water Yield of North Korean Forests. *Forests* **2020**, *11*, 804. [[CrossRef](#)]
46. Mishra, S.K.; Singh, V.P. *Soil Conservation Service Curve Number (SCS-CN) Methodology*; Springer Science & Business Media: Berlin/Heidelberg, Germany, 2013.
47. Mishra, S.K.; Singh, V.P. A relook at NEH-4 curve number data and antecedent moisture condition criteria. *Hydrol. Process.* **2006**, *20*, 2755–2768. [[CrossRef](#)]
48. Hjemfelt, A., Jr.; Kramer, L.; Burwell, R. Curve numbers as random variables. In *Rainfall-Runoff Relationship*; Water Resources Publications: Littleton, CO, USA, 1982; Volume 4, pp. 365–370.
49. Wang, S.; Zhang, X.; Wang, C.; Zhang, X.; Reis, S.; Xu, J.; Gu, B. A high-resolution map of reactive nitrogen inputs to China. *Sci. Data* **2020**, *7*, 379. [[CrossRef](#)] [[PubMed](#)]
50. Chiarelli, D.D.; Passera, C.; Rosa, L.; Davis, K.F.; D'Odorico, P.; Rulli, M.C. The green and blue crop water requirement WATNEEDS model and its global gridded outputs. *Sci. Data* **2020**, *7*, 273. [[CrossRef](#)]
51. Costanza, R.; de Groot, R.; Sutton, P.; van der Ploeg, S.; Anderson, S.J.; Kubiszewski, I.; Farber, S.; Turner, R.K. Changes in the global value of ecosystem services. *Glob. Environ. Chang.* **2014**, *26*, 152–158. [[CrossRef](#)]
52. Morse-Jones, S.; Luisetti, T.; Turner, R.K.; Fisher, B. Ecosystem valuation: Some principles and a partial application. *Environmetrics* **2011**, *22*, 675–685. [[CrossRef](#)]
53. Schaefer, M.; Goldman, E.; Bartuska, A.M.; Sutton-Grier, A.; Lubchenco, J. Nature as capital: Advancing and incorporating ecosystem services in United States federal policies and programs. *Proc. Nat. Acad. Sci. USA* **2015**, *112*, 7383–7389. [[CrossRef](#)]
54. Sterling, S.M.; Ducharme, A.; Polcher, J. The impact of global land-cover change on the terrestrial water cycle. *Nat. Clim. Chang.* **2013**, *3*, 385–390. [[CrossRef](#)]
55. Ellison, D.; Morris, C.E.; Locatelli, B.; Sheil, D.; Cohen, J.; Murdiyarto, D.; Gutierrez, V.; Noordwijk, M.V.; Creed, I.F.; Pokorny, J.; et al. Trees, forests and water: Cool insights for a hot world. *Glob. Environ. Chang.* **2017**, *43*, 51–61. [[CrossRef](#)]
56. Burkhard, B.; Kroll, F.; Nedkov, S.; Müller, F. Mapping ecosystem service supply, demand and budgets. *Ecol. Indic.* **2012**, *21*, 17–29. [[CrossRef](#)]
57. Talukdar, S.; Singha, P.; Shahfahad; Mahato, S.; Praveen, B.; Rahman, A. Dynamics of ecosystem services (ESs) in response to land use land cover (LU/LC) changes in the lower Gangetic plain of India. *Ecol. Indic.* **2020**, *112*, 106121. [[CrossRef](#)]
58. Zhang, L.; Cheng, L.; Chiew, F.; Fu, B. Understanding the impacts of climate and landuse change on water yield. *Curr. Opin. Environ. Sustain.* **2018**, *33*, 167–174. [[CrossRef](#)]
59. Chatterjee, S.; Dutta, S.; Dutta, I.; Das, A. Ecosystem services change in response to land use land cover dynamics in Paschim Bardhaman District of West Bengal, India. *Remote Sens. Appl. Soc. Environ.* **2022**, *27*, 100793. [[CrossRef](#)]
60. Adham, M.I.; Shirazi, S.M.; Othman, F.; Rahman, S.; Yusop, Z.; Ismail, Z. Runoff Potentiality of a Watershed through SCS and Functional Data Analysis Technique. *Sci. World J.* **2014**, *2014*, 379763. [[CrossRef](#)] [[PubMed](#)]
61. Rawat, K.S.; Singh, S.K.; Szilard, S. Comparative evaluation of models to estimate direct runoff volume from an agricultural watershed. *J. Geol. Ecol. Landsc.* **2021**, *5*, 94–108. [[CrossRef](#)]
62. Li, M.; Li, S.; Liu, H.; Zhang, J. Balancing Water Ecosystem Services: Assessing Water Yield and Purification in Shanxi. *Water* **2023**, *15*, 3261. [[CrossRef](#)]
63. Bangash, R.F.; Passuello, A.; Sanchez-Canales, M.; Terrado, M.; López, A.; Elorza, F.J.; Ziv, G.; Acuña, V.; Schuhmacher, M. Ecosystem services in Mediterranean river basin: Climate change impact on water provisioning and erosion control. *Sci. Total Environ.* **2013**, *458–460*, 246–255. [[CrossRef](#)]

64. PGHP. Hainan FTP: Key Industrial Parks Take in ¥2 Trillion in 2023. Available online: <https://en.hainan.gov.cn/englishgov/Photos/202402/440ccc318bef45ef8558f7f46401a6c0.shtml?> (accessed on 3 May 2024).
65. Zhang, Q.; Chu, Y.; Xue, Y.; Ying, H.; Chen, X.; Zhao, Y.; Ma, W.; Ma, L.; Zhang, J.; Yin, Y.; et al. Outlook of China's agriculture transforming from smallholder operation to sustainable production. *Glob. Food Secur.* **2020**, *26*, 100444. [[CrossRef](#)]

Disclaimer/Publisher's Note: The statements, opinions and data contained in all publications are solely those of the individual author(s) and contributor(s) and not of MDPI and/or the editor(s). MDPI and/or the editor(s) disclaim responsibility for any injury to people or property resulting from any ideas, methods, instructions or products referred to in the content.